Title
Perovskite Solar Cells for Photoelectrochemical Water Splitting and CO_2 Reduction

Authors
Gurudayal
Ager, Joel
Mathews, Nripan

Publication Date
2018-10-29

DOI
10.1002/9783527800766.ch4_02

Peer reviewed

2.2 Perovskite Solar Cells for Photoelectrochemical Water Splitting and CO_2 Reduction

Gurudayal, Joel Ager, Nripan Mathews

1. Introduction

Rapid economic and demographic changes continue to increase the world's dependence on fossil fuels as an energy source. Urbanization and further increase in population will serve to accelerate the trend. Fossil fuels meet more than 80% of the total primary energy demand and generate over 90% of the primary greenhouse gases: (CO_2), methane (CH_4) and nitrous oxide (N_2O).[1] The current atmospheric CO_2 level is more than 400 ppm, which is significantly higher compared to pre-industrial times, and continues to rise.[2] In principle, energy provided by the sun has the potential to meet our energy demand. However, it is a significant technological challenge to convert and store solar energy by efficient and cost effective methods on a large scale. While conversion of solar light to power via photovoltaic panels has grown rapidly, the temporal intermittency of the source, as well as its uneven geographical distribution, will ultimately limit its ability to displace fossil fuels.

Storing solar energy in the form of fuels would be advantageous and environmentally friendly, if it could be done efficiently.[3, 4] Photoelectrochemical (PEC) water splitting is inspired from the natural photosynthesis process in plants, where solar energy is captured and converted into hydrocarbons, glucose and oxygen.[5, 6] Indeed, there is considerable research effort into "artificial photosynthesis," or photoelectrochemical (PEC) methods to convert solar energy to chemical fuels such as hydrogen and hydrocarbons.[6, 7] Considering the case of hydrogen, it can be generated by splitting of water by reaction (1).

$$2H_2O + Light \rightarrow 2H_2 + O_2 \quad \Delta E = 1.23\,V\ vs\ RHE \quad (1)$$

The half reactions are

$$H_2O + light \rightarrow 2H^{+} + \frac{1}{2}O_2 + 2e^{-}$$

$$2H^{+} + 2e^{-} \rightarrow H_2$$

The overall ΔE^0 is 1.23 eV, while an overpotential (0.4-0.6 eV) is required to overcome the thermodynamic and recombination losses associated with the reaction.[8, 9, 10, 11] Hydrogen is an attractive fuel because it has high gravimetric energy density, nearly three times that of gasoline.[12] PEC generated hydrogen can be utilized as an energy source by converting it to electricity in a fuel cell.[13, 14] However, generating such chemical potential difference by solar absorption in a single semiconductor photoelectrode is challenging. At least two semiconductors in tandem with complimentary absorption spectrum and appropriate conduction and valence band positions with respect to water redox levels are required to efficiently harvest the solar energy and drive water-splitting reaction.[15, 16]

Carbon dioxide (CO_2) is an alarming greenhouse gas and anthropogenic increases in its concentration are the major driver for global warming. To conserve environmental stability, CO_2 produced on Earth should balance consumption. Sustainable CO_2 reduction to form fuels would thus be able to tackle two environmental challenges concurrently. CO_2 conversion can be achieved by electrochemical and photoelectrochemical reactions. However, CO_2 capture, conversion, and utilization requires high energy, appropriate selective catalysts that make this reaction more challenging. Electrochemical CO_2 reduction involves multi-electron transfer and can produce either gaseous (CO, CH_4, C_2H_4) or liquid fuels (HCOOH, CH_3OH, CH_3CH_2OH etc.) The thermodynamic electrochemical half-reactions of CO_2 reduction with their standard electrode potentials are as follows:

$$CO_2+4H^+¿+4e^-¿\rightarrow C+2H_2OE_0=0.210V\ vs\ SHE(2)¿¿$$

$$CO_2+2H^+¿+2e^-¿\rightarrow CO+H2OE_0=-0.103V\ vs\ SHE(3)¿¿$$

$$CO_2+8H^+¿+8e^-¿\rightarrow CH_4+2H_2OE_0=0.169V\ vs\ SHE(4)¿¿$$

$$2CO_2+12H^+¿+12e^-¿\rightarrow C_2H_4+4H_2OE_0=0.079V\ vs\ SHE(5)¿¿$$

$$CO_2 + H^+ + 2e^- \rightarrow HCOO^- \quad E_o = -0.225\,V\,vs\,SHE \quad (6)$$

$$CO_2 + 2H^+ + 2e^- \rightarrow HCOOH \quad E_o = -0.250\,V\,vs\,SHE \quad (7)$$

$$CO_2 + 6H^+ + 6e^- \rightarrow CH_3OH + H_2O \quad E_o = 0.016\,V\,vs\,SHE \quad (8)$$

$$CO_2 + 12H^+ + 2e^- \rightarrow CH_3CH_2OH + 3H_2O \quad E_o = 0.084\,V\,vs\,SHE \quad (9)$$

When coupled to reaction (1a), which will yield a source of electrons via oxidation of water, it is possible to imagine the use of reactions (2)-(9) as a sustainable method to reduce CO_2 to fuels. It is to be noted that the all the reactions are within 225 mV of the potential for H_2 evolution (HER), reaction (1a), which is 0 V vs. SHE at standard conditions. Thus, HER competes with the CO_2 reduction reaction (CO_2RR) in aqueous solution.

1.1. Photoelectrochemical generation of H_2

Hydrogen generation from photoelectrochemical (PEC) cells through water splitting is a well-established concept.[5, 8, 13] However, primary challenges include improvement of the water splitting efficiency and stability. [11, 17],[18] In a water splitting PEC cell, water molecules are broken into hydrogen at the cathode/ semiconductor photocathode and oxygen at the anode/semiconductor photoanode. When a semiconducting photo-electrode is immersed in an electrolyte solution, charge transfer occurs between the semiconducting electrode and the electrolyte until the equilibrium condition is achieved (Figure 1).[19, 20] For an n-type semiconductor, typically upward band bending occurs at the surface of electrode to match the Fermi level of the semiconductor and the redox level of the electrolyte. Similarly, downward band bending occurs at the surface of the electrode to match the Fermi level of a p-type semiconductor and the redox level of the electrolyte.

A depletion layer or a space-charge layer exists at the interface of the semiconductor and electrolyte. Under illumination, the electric field in the space charge layer is useful for the separation of photo-generated electron and hole pairs. Figure 1 shows the energy levels of isolated and submerged n/p-type semiconducting photo-electrodes and the redox potentials of the redox species in the electrolyte. The overall water splitting reaction, water reduction and oxidation driven by photo-generated electron and holes are represented by the following reaction schematic;[15, 21]Although there has been significant development to make efficient PEC cells for hydrogen production, there still exists a big gap between the achieved and theoretically predicted efficiencies of PEC cells.[11, 16, 22, 23]

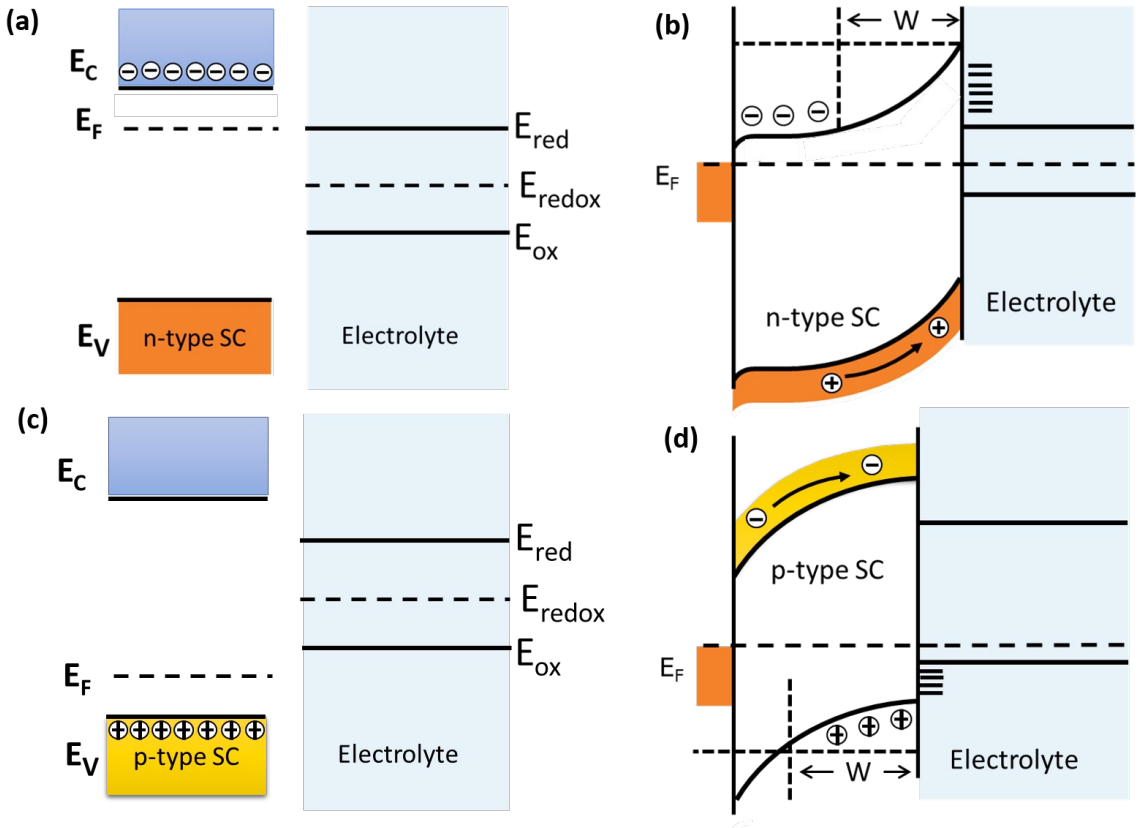

Figure 1 (a) The isolated energy band diagram of the n-type semiconductor and the electrolyte, **(b)** The equilibrated energy band diagram and the formation of space charge layer in n-type semiconductor when it is immersed in to the electrolyte, **(c)** The remote energy band diagram of the p-type semiconductor and

the electrolyte, and **(b)** The equilibrated energy band diagram and the formation of space charge layer in p-type semiconductor when it is immersed in to the electrolyte.

1.2. PEC electrode materials

It remains a challenge to find a material, which can oxidize and reduce water without any external bias.[24] PEC electrode materials should have good aqueous stability, appropriate band levels with respect to water redox levels, high optical absorption in visible range and good electrical properties.[25] Many semiconducting materials for solar water splitting have been explored, but either the position of conduction and valence band are not favorable for both water reduction and oxidation potential simultaneously, or the ones that do have too large a bandgap to generate effective photocurrents (Figure 2).[26] Metal oxides are relevant for PEC water splitting, mainly due to their semiconducting properties, stability in aqueous solutions and reasonably low cost.[20, 26-29] However, most of metal oxides have wide energy band gap and poor semiconducting properties in comparison with traditional III-V semiconductors and Silicon.[21, 27]

Among all metal oxide semiconductor oxides, TiO_2 has attracted much attention owing to its band levels, but high-energy band gap and inefficient absorption of sunlight spectrum has limited its performance.[30, 31] To tackle this problem, dyes with high visible light absorption capability, were utilized with limited success.[31, 32] Bismuth vanadate ($BiVO_4$) is another material explored for PEC water splitting, however its STH efficiency is limited by its band gap (2.4 eV), and poor stability.[33, 34] There have been major developments in the preparation of oxynitride materials (TaON and Ta3N5), which have an optimum energy band gap and can drive both water oxidation and reduction but the reported quantum efficiency (~ 5-6 %) is still low.[35] Out of the various candidates explored, the most promising stable photocurrents reported to date was achieved using Iron (III) oxide i.e. Fe_2O_3

or hematite.[21, 36] Iron (III) oxide shows largely favorable properties for water-splitting; however has an unfavorable conduction band level to reduce water necessitating the application of an external bias.[37]

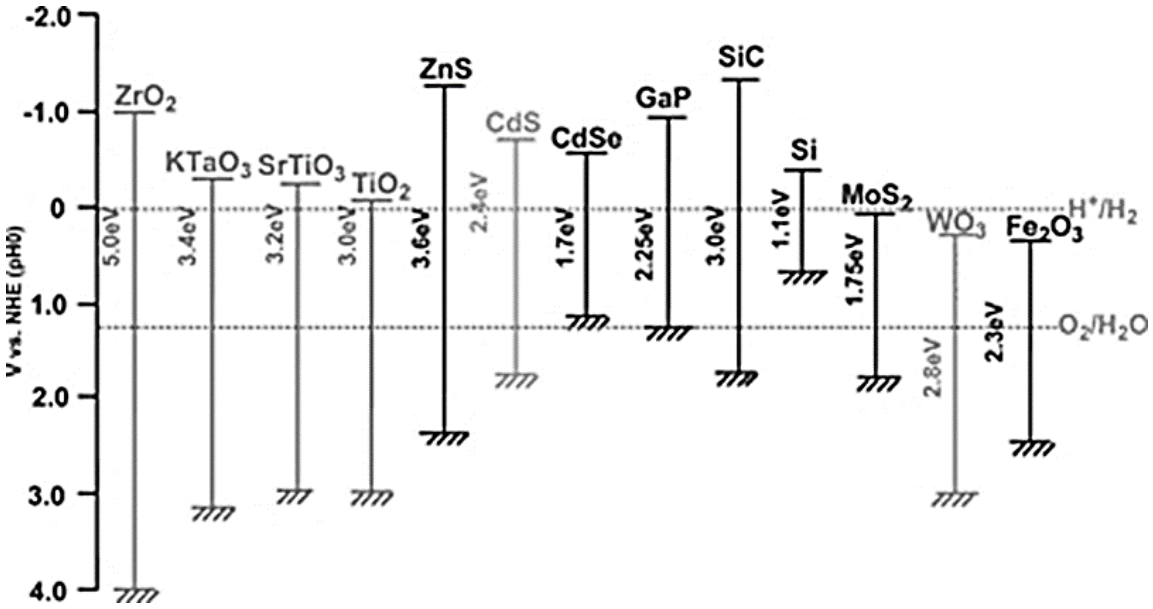

Figure 2. The band edge positions of different photoelectrodes with water oxidation/reduction potential.[29] Reprinted with the permission of Royal Society of Chemistry 2009.

In addition to the challenges of stability, poor energy level alignment of the photoelectrodes with respect to water redox levels, the energy required for water splitting is significantly higher than the thermodynamic potential (1.23 eV) because of loss processes within the PEC cell. Furthermore, the additional voltage is required to overcome the overpotentials, resulted from the kinetic barriers of the intermediate species involved in the water oxidation and reduction mechanisms. The four-electron process for the oxygen evolution reaction (OER) demands even higher overpotential (0.3-0.5 eV) for a reasonable current density (~ 10mAcm^{-2}). Accordingly, a single photo-absorbing material is not enough to generate the required photopotential to split water without an external bias.

In the following section, we discuss the approach to combine materials in a PEC cell and fabricate a tandem cell. Here, we distinguish a few commonly used approaches for bias free water splitting.[38]

2. Tandem Configurations

Tandem approaches for solar to hydrogen conversion have been reviewed recently.[18, 39, 40] There are a number of demonstrations of overall water splitting tandem cells with decent solar to hydrogen conversion efficiency reported from different groups.[16, 24, 40-44]

In tandem cell configurations (Photoelectrochemical cell-photovoltaic and photoanode-photocathode), the total photovoltage is produced by complementary optical absorption in two or more photoabsorbers connected in series to split water efficiently (Figure 3).[15, 16, 24, 44-46] Whereas the most simplest and reliable approach is electrochemical-photovoltaic (EC-PV) configuration (Figure 3(c)). Additionally, it is hard to realize a single photoelectrode or photoanode-photocathode system to perform both OER and HER in the same pH electrolyte solution. For PEC-PV configuration, the photovoltage outputs of the sub-cells are crucial, especially the photovoltage generated by traditional solar cells i.e., silicon, CIGS and DSSC is not enough to drive water splitting reaction.[24, 45, 47] In this context, the relatively large open circuit voltages of the halide perovskite solar cells have made them attractive candidates as the photovoltaic components of solar fuel devices.[16, 41, 42, 44] The multiple light absorber tandem PEC systems can easily harvest a significant portion of the solar spectrum and generate enough voltage to overcome the overpotential and thermodynamical potential for water splitting. In the subsequent sections, different systems using multi photoabsorbers will be deliberated. Finally, a balance between the system complexity, cost, and solar to hydrogen (STH) conversion efficiency will be discussed.

For large scale applications, a PEC device should cost less than US$ 160 per m^2 with a STH efficiency of 10%.[4] To achieve this target, a PEC cell must be

composed of abundant environment friendly materials combined with facile, cost-effective and scalable fabrication techniques to meet the high throughputs required of the PEC device.[4, 44]

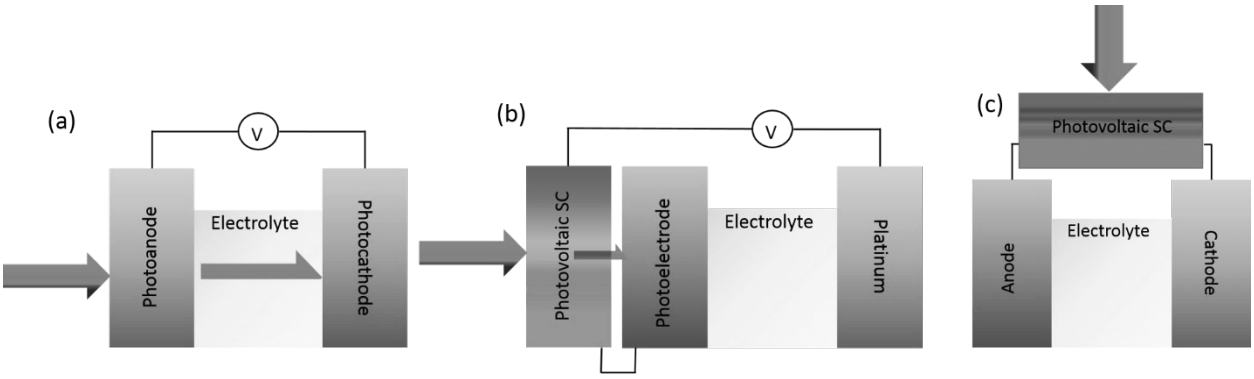

Figure 3. Tandem cell configurations, (a) photoanode-photocathode system, (b) photoelectrode-PV configuration, and (c) photovoltaic-electrocatalyst structure.

2.1. Photoanode-Photocathode Strategy

The photoanode-photocathode tandem devices drive two separate water redox half-reactions in a PEC cell. The p-type photocathode/n-type photoanode tandem system is the simplest and straightforward in terms of materials availability, fabrication cost and synthesis. The photoelectrodes can be fabricated separately and subsequently wired to each other, or fabricated on the same substrate with local interconnection. The typical energy band diagram of photoanode-photocathode tandem system is shown in Figure 4. In addition to appropriate conduction and valence band edges to the water redox levels, the materials must have complimentary absorption spectra as well. However, this approach is under-explored in literature due to the additional challenge of driving both the water redox reactions at the same pH electrolyte solution. This challenge necessitates the development of robust protection layers. Most importantly, the energy band alignment of photoelectrodes is critical to achieve a notable STH efficiency. Turner et al

showed the importance of band alignment by fabricating a device of $GaInP_2$ (E_g ~ 1.83 eV) photocathodes in tandem with either WO_3 or Fe_2O_3 photoanodes under light illumination (more than 200 $mWcm^{-2}$).[48, 49] Whereas, the WO_3/$GaInP_2$ tandem produced a detectable photocurrent 20 $\mu A\ cm^{-2}$ at 1000 $mW\ cm^{-2}$. While, Fe_2O_3/$GaInP_2$ tandem system produced negligible photocurrent even at 10 sun illumination because of mismatch of the conduction band minimum of the Fe_2O_3 thin film and the valence band maxima of $GaInP_2$ (Figure 5 (a) and (b)). Gopal et al demonstrated a tandem cell of improper band alignment, which is fabricated by a p-type Cu–Ti–O nanotube array photocathode in series with n -type TiO_2 photoanode.[50] This tandem configuration shows a small STH efficiency of 0.3%, which is because of similar absorption spectra of both materials.[50] Lai et al. investigated TiNi treated p-type Si photocathode/TiCo coated WO_3 photoanode and TiNi treated p-type Si/ TiCo coated $BiVO_4$ photoanode PEC tandem systems for unassisted water splitting.[51] TiNi treated p-Si photocathode and TiCo coated $BiVO_4$ photoanode achieved unassisted water splitting STH efficiency of 0.05%, whereas the p -TiNi/Si photocathode and TiNi/WO_3 photoanode did not show any activity. This unpredicted performance resulted from the 0.3 V higher CB position of $BiVO_4$ compared to WO_3, which might change the absorption spectrum matching and generate higher photovoltage and operating photocurrent.[51]

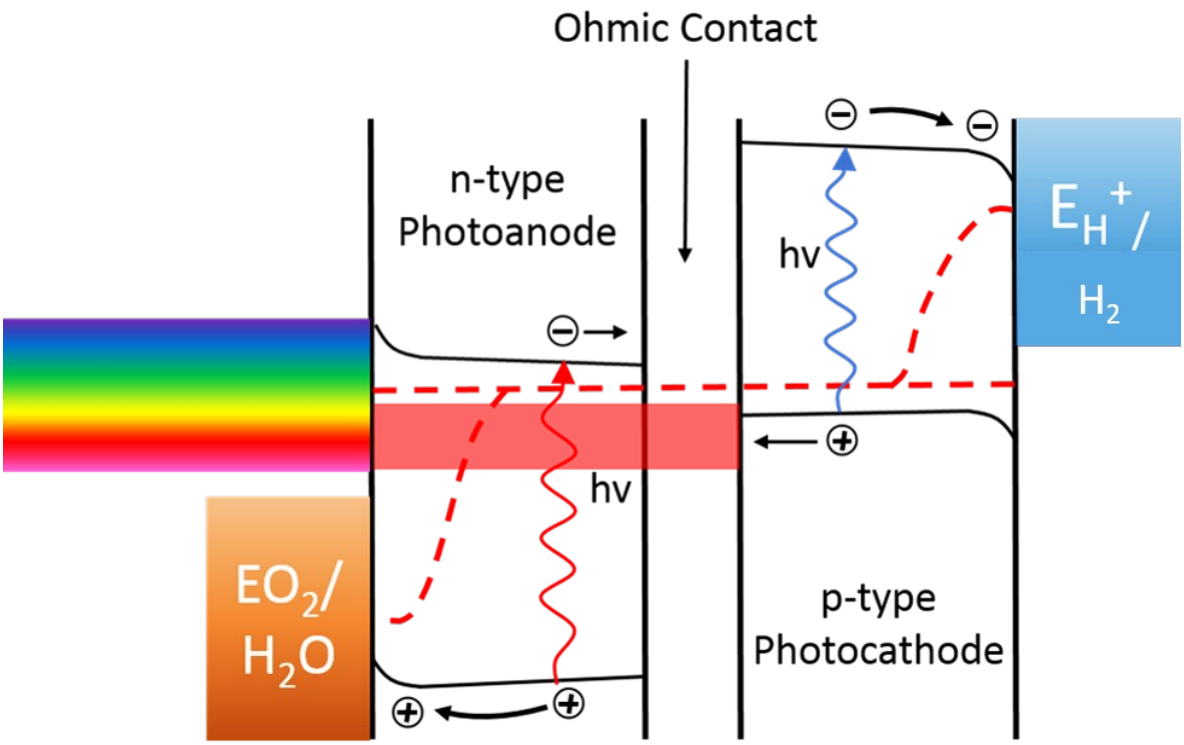

Figure 4. The schematic of energy band diagram of a photoanode-photocathode tandem cell.

Although, there are other factors involve except band alignment to improve the STH efficiency. Nozik et al fabricated an n-TiO_2/p-GaP tandem cell, which shows both hydrogen and oxygen evolution without any external bias voltage. However, the high internal series resistance limited the solar to hydrogen conversion efficiency of 0.25% at zero bias. The device stability was also poor due to oxide layer formation on the surface of the p-GaP.[19] Liu et al. demonstrated a photoanode-photocathode tandem system of n-type TiO_2 / p-type Si for unassisted water splitting that accomplished a solar to hydrogen conversion (STH) efficiency 0.12%. [52] Again, the limited STH efficiency was due to the high-energy band gap of TiO_2 and ohmic losses in the device. Ding et al. demonstrated a FeOOH overlayer coated $BiVO_4$ photoanode and Pt treated Si photocathode tandem cell, where both the photoelectrodes are parallelly illuminated and exhibiting a STH efficiency of

2.5%.[53] [54] A $BiVO_4/Cu_2O$ tandem cell fabricated by Bornoz et al showed a maximum STH efficiency of 0.5% (Figure 5 (c) and (d)) despite a high theoretical STH efficiency of 8% with the rear Cu_2O photocathode expected to absorb all photons of wavelengths between 500 nm to 620 nm.[55] A p-type $CaFe_2O_4$ photocathode in tandem with n-type TiO_2 (parallel configuration) to generate an operating current density of 110 μAcm^{-2} in 0.1M NaOH electrolyte solution.[56] This device was unstable and the Faradaic efficiency for gas evolution was observed to be only 12%, which is uncertain. Jang et al. showed PEC tandem cells comprises of NiFeOx overlayer coated hematite photoanode and a p-type Si photocathode in tandem, with STH efficiency of 0.91% (Figure 6 (a-c)). Kim et al., reported another tandem configuration of a $Pt/CdS/CuGa_3Se_5/(Ag,Cu)GaSe_2$ photocathode and NiOOH/FeOOH/Mo doped $BiVO_4$ photoanode, which exhibit a STH conversion efficiency of 0.67% (Figure 6 (d-f)).[57]

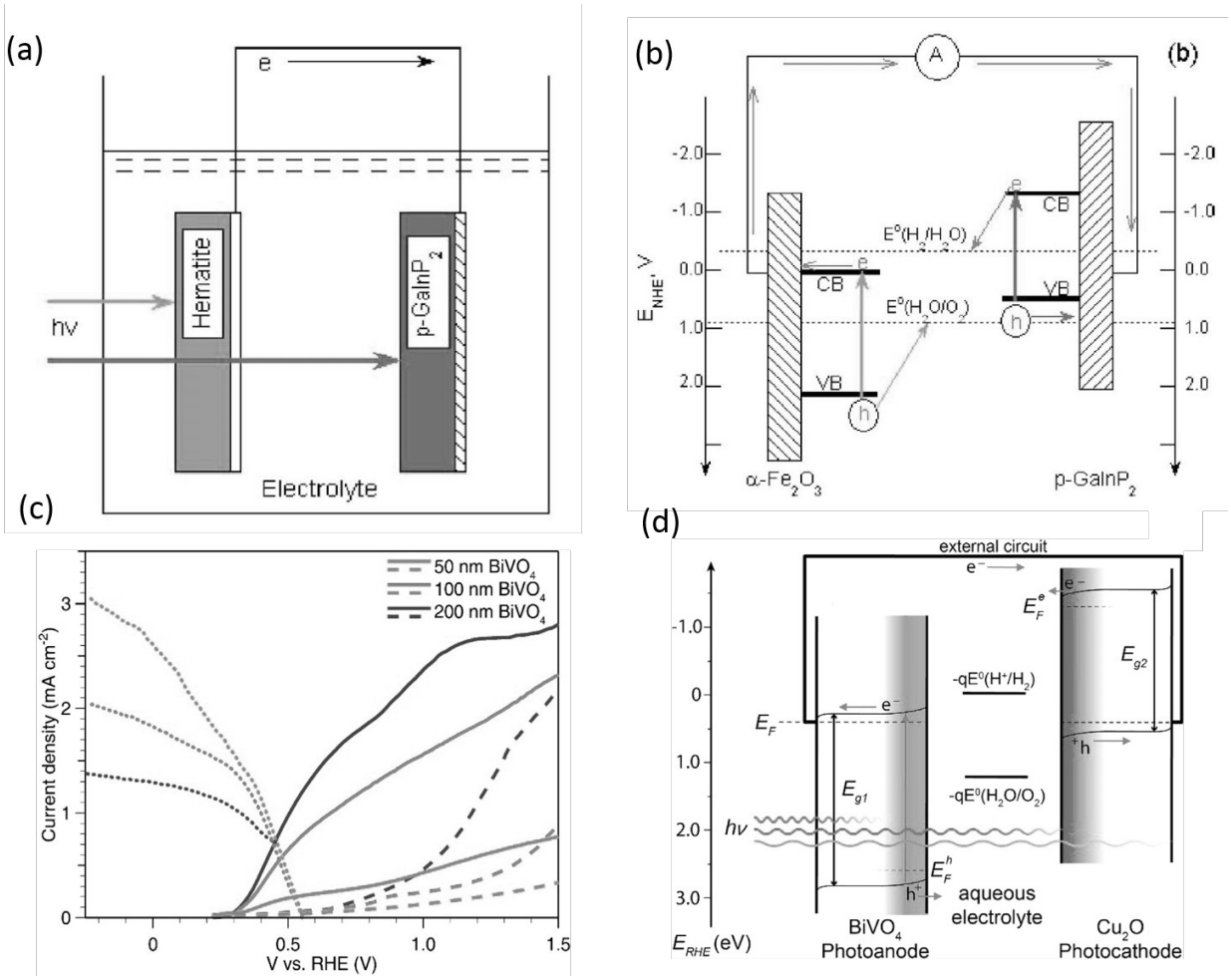

Figure 5. (a) Schematic of hematite and $GaInP_2$ tandem cell, (b) Energy diagram of a hematite photoanode and $GaInP_2$ photocathode tandem cell for unassisted water splitting. Reprinted with the permission of Journal of the Electrochemical society.[49] Copyright 2008. (c) J–V curves for the CoPi/$BiVO_4$ photoanodes and Cu_2O photocathode under simulated solar illumination (100 $mWcm^{-2}$), and (d) Energy diagram of a $BiVO_4$ photoanode and Cu_2O photocathode tandem cell for unassisted water splitting. Reprinted with the permission.[55] Copyright 2014, American Chemical Society.

Above mentioned tandem devices suffered from the low STH efficiencies, which is due to the absorption mismatch and slow redox kinetics. These results a low photopotential generation, which is insufficient to overcome the overpotential and thermodynamic potentials of water splitting. Theoretical

study predicted to achieve a maximum STH efficiency of 29.7% from this configuration however it's very far from what we have achieved till date.[39] The main challenge is the lack of materials availability with the suitable energy band gap to harvest visible spectrum and appropriate band edge positions with respect to appropriate water redox potentials. Detailed calculation of energy band edges of photoelectrodes required in tandem configuration were reported by Lewis et al.[39]

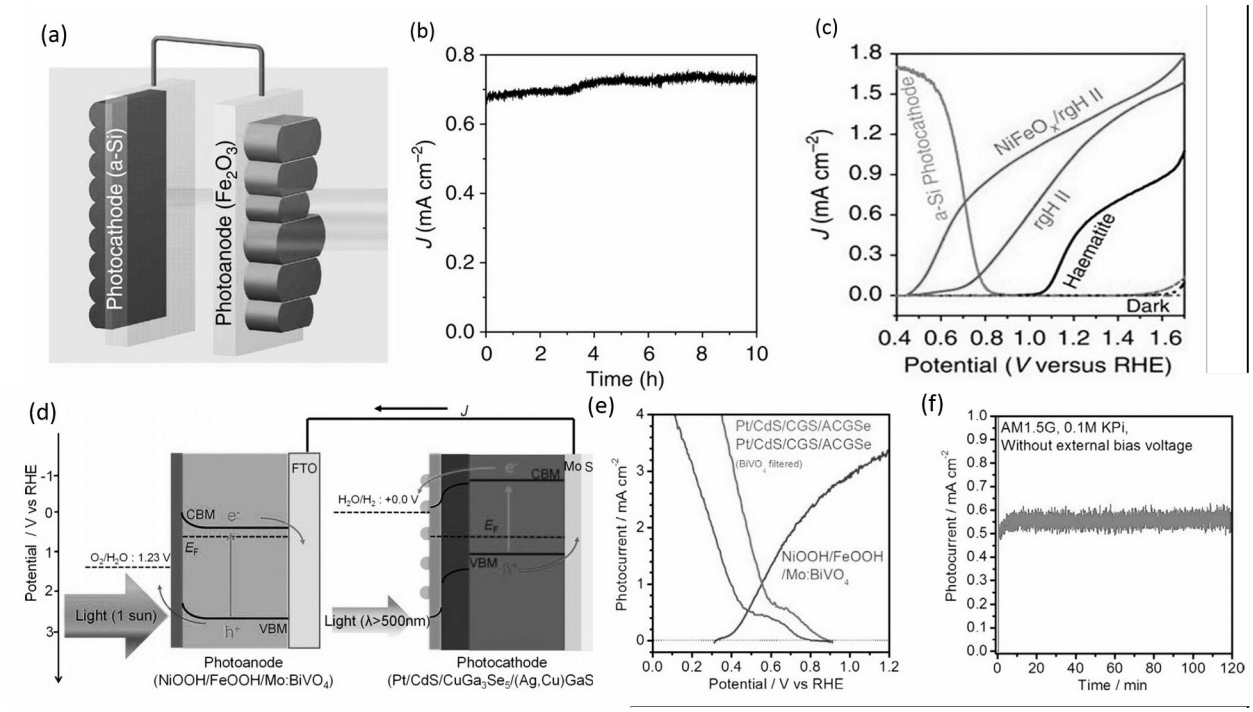

Figure 6. (a) Schematic of a photoanode-photocathode tandem cell with an amorphous Si photocathode and hematite photoanode. (b) Stability curve of a-Si – hematite tandem cell, and (c) J–V curves of hematite coated with an OER catalyst (NiFeOx). Reproduced with permission.[58] Copyright 2015, Nature Publishing Group. (d) Schematic of NiOOH/FeOOH/Mo:$BiVO_4$ photoanode and Pt/CdS/CGS/ (Ag,Cu)$GaSe_2$ photocathode tandem cell for overall water splitting, (e) J-V curves of photoanode (NiOOH/FeOOH/Mo:$BiVO_4$) and photocathode (Pt/CdS/CGS/$GaSe_2$) against applied potential for parallel and tandem scheme. (f) Stability curve for the tandem PEC cell. Reproduced with permission.[57] Copyright 2016 Wiley Online Library.

2.2. PEC- PV Tandem system

The PEC-PV tandem approach is more advantageous than PEC alone because a single photoabsorber unable to produce the required photovoltage to drive water splitting reaction. This approach has been explored widely in literature, in which a photoanode or a photocathode is connected in series (wired or stacked) with a single or multiple junction solar cells. The photoelectrode and photovoltaic solar cells with complimentary absorption spectra connected in series generates enough photopotential to exceed the overpotential and thermodynamic potential to drive water splitting. The ohmic contact between the photoelectrode and PV can be performed via a conducting metal wire or a transparent conductive oxide for wireless monolithic configurations.[16, 42] The wired configuration is convenient for assembling the components, whereas the wireless monolithic configuration is more appropriate for scalable development. While, most of the wireless devices reported till date suffered from the stability issues.[22]

A widely recognized PEC-PV configuration was demonstrated by Turner *et al*., consisting of a monolithic epitaxially grown III-V semiconductor system with a GaAs pn-junction coupled to a $GaInP_2$ photocathode. This device exhibited an impressive solar to hydrogen (STH) conversion efficiency of 12.5%, however the system suffered from stability issues due to corrosion of the $GaInP_2$ photocathode in contact with the aqueous electrolyte solution.[22] An additional drawback of this system is the high costs associated with its fabrication. Different tandem illumination configurations have been reported with similar performance and better light harvesting. While designing a tandem system for efficient water splitting, the choice of the photoelectrodes is critical. The actual device was first realized by Park and Bard in 2006, who reported that a 1.9% STH efficiency was achieved under 1 sun illumination. [59] Park's group improved the STH efficiency of an integrated WO_3 /DSSC to approximately 2.1% using a mesoporous WO_3 photoanode in 1 M H_2SO_4

electrolyte.[60] Gratzel's group demonstrated a simple yet cost effective DSSC-WO_3 and DSSC-Fe_2O_3 PEC-PV tandem cell with a STH efficiency of 3.1% and 1.7% respectively.[24] Furthermore, Shin and Park reported a transparent TiO_2 nanotube photoanode loaded with CdS/CdSe particles, with an STH efficiency of 2.1% STH efficiency.[61] Shi et al. also demonstrated a FeOOH/NiOOH $BiVO_4$/mesoporous WO_3 photoanodes and a DSSC PV in tandem configuration, which shows a 5.7% STH efficiency.[61] This PEC-PV tandem cell was assembled through a transparent double-sided conductive glass substrate in a wireless configuration.[61] The introduction of $BiVO_4$ improved solar light harvesting of the visible ranges compared with the conventional WO_3 photoanode, and the water redox kinetics could be further enhanced with the loading of a co-catalyst (FeOOH/NiOOH). Fatwa et al fabricated tandem devices using gradient-doped $BiVO_4$ integrated with double-junction amorphous Si PV cells in wired or wireless configurations, which reached 5.2% and 4.9% STH efficiency, respectively.[45, 62]

Multijunction PV cells were heavily utilized for light harvesting compared with single PV cells in PEC-PV tandem cells. Due to the low open circuit voltages of conventional photovoltaic systems (Si, CuInGaS/Se, DSSC), many of the tandem designs have required the series integration of several solar cells to generate the photopotential required for splitting water.[24, 34, 45, 47] These complicated approaches require a careful balance of the optical absorption and photocurrent generation within each solar cell to drive the overall reaction efficiently. Moreover, such architectures should also balance performance against fabrication complexity in order to allow for economical solar hydrogen production. Perovskite solar cells are revolutionary due to their facile fabrication, their high open circuit voltage (1.1 V to 1.4 V) which is advantageous to drive solar assisted water splitting reaction with a single photoabsorber. The superb light-harvesting characteristics of perovskite materials in the solar-cell research field have led to a rapid increase in power conversion efficiency.[44, 63] Figure 7 shows a notable example of a hematite

PEC electrode integrated with one rear perovskite PV cell. In this case, the PV cell provides a bias between the photoanode and counter electrode (commonly Pt) when illuminated. O_2 gas will be generated from the photoanode surface, and H_2 evolution will occur at the Pt surface.

In 2013, we have successfully demonstrated a $CH_3NH_3PbI_3$ (Eg = 1.55 eV) perovskite PV cell in a PEC/ PV tandem cell with a Fe_2O_3 photoanode for unassisted water splitting, resulting in a 2.4% STH efficiency in 1 M NaOH electrolyte.[42] Our PEC-PV tandem device contained a single perovskite solar cell and a Mn-doped hematite photoanode, as shown in Figure 7. However, the PEC-PV tandem device still suffers from poor overall photocurrent density due to the low photocurrents produced by the thin Fe_2O_3 photoanode even after Mn doping. Kim et al. demonstrated a cobalt carbonate (Co–Ci) catalyst modified $BiVO_4$ photoanode with a single $CH_3NH_3PbI_3$ perovskite solar cell. This photoanode/perovskite tandem cell was encapsulated by epoxy for protection against corrosion and shown in Figure 8.[16] This device exhibit a STH efficiency of 4.3% in wire configuration and 3.0% in wireless configuration, with an excellent stability of 10 h.[16] Kamat's group successfully fabricated a $CH_3NH_3PbI_3$ perovskite solar-cell based PEC-PV tandem cell using $BiVO_4$ photoanode, which yielded 2.5% STH efficiency (Figure 9).[43] A similar demonstration of perovskite solar cell and $TiO_2/BiVO_4$ photoanode tandem cell with a STH efficiency of 1.24%.[64] There are few interesting demonstrations of perovskite/photocathode devices from various groups and those are also promising for unassisted water splitting. Dias et al. demonstrated a perovskite $CH_3NH_3PbI_3$-PEC tandem cell with r an STH η of 2.5%.[46], whereas the PEC cell consisting a p-type Cu_2O photocathode and IrO_2 anode. The transparency of Cu_2O photocathode was optimized by a thin gold underlayer, Cu_2O has a bandgap (2.1 eV) and utilized as a top absorber component, whereas the $CH_3NH_3PbI_3$ (1.1 eV) used as a bottom absorber. Other notable work include an inverted PEC-PV tandem cell configuration,

where a perovskite large band gap $CH_3NH_3PbBr_3$ (Eg = 2.3 eV) PV cell was placed in tandem with a smaller bandgap $CuIn_xGa_{1-x}Se_2$ layer (Eg = 1.1 eV) which functioned as the photocathode.[41] This device exhibits an STH efficiency of 6.3% due to the proper energy band gap alignment, which enabled efficient harvesting of the solar spectrum. However, the $CH_3NH_3PbI_3$ solar cell tandem device shows only 2.6% STH efficiency, which is because of high absorbability of the $CH_3NH_3PbI_3$ in comparison of $CH_3NH_3PbBr_3$. The inverted PEC-PV tandem cell has the potential to further improve the STH efficiency, when it's in tandem with small energy band gap photoelectrodes. [41] The greatest advantage of using halide perovskite is it's bandgap tunability (1.1–2.3 eV), which allows to choose a wide variety of photoelectrodes. However, the perovskite solar cell must be immersed in a water electrolyte, which induces an inherent stability problem. As a result, these perovskite-based PEC-PV tandem devices without protection layer cannot be operated for longer period of time. Numerous demonstrations of perovskite PV-PEC tandem devices have been shown recently (Figure 10).

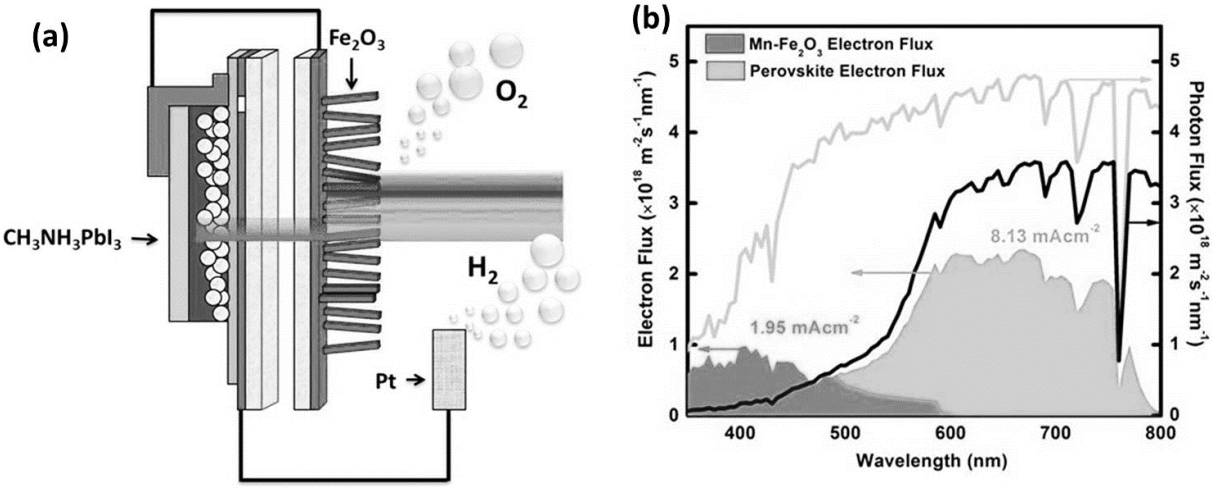

Figure 7. Hybrid photovoltaic and photoelectrosynthetic approach of Guru et al. 98for overall water splitting with an efficiency of 2.4%. A $CH_3NH_3PbI_3$ cells was used

to bias an oxygen evolving Fe_2O_3 photoanode. Reproduced with permission.[42] Copyright 2015 American Chemical Society.

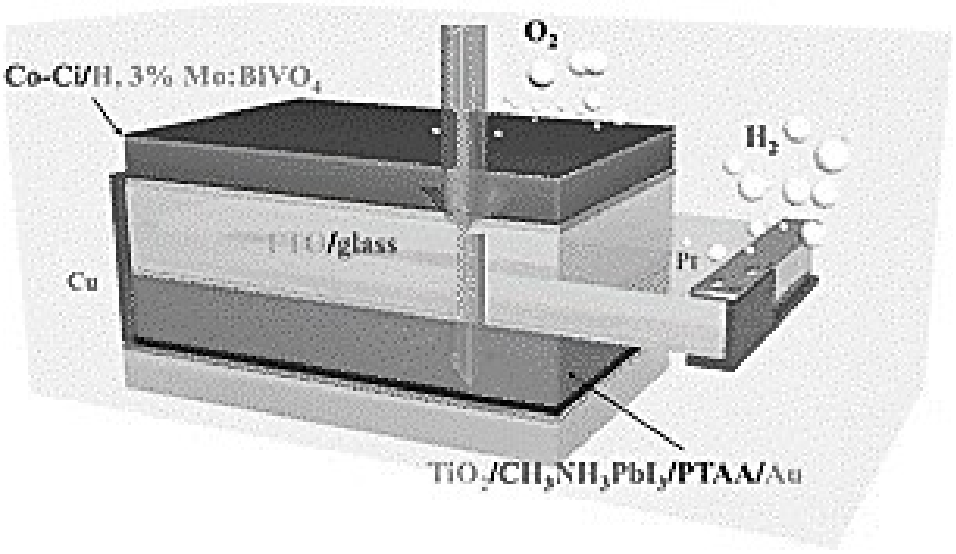

Figure 8. Wireless photoelectrosynthetic approach of Kim et al. 100 for overall water splitting with an efficiency of 3%. A $CH_3NH_3PbI_3$ cell was used in optical and electrical series with a Mo-doped $BiVO_4$ photoanode. Reproduced with permission.[16] Copyright 2015 American Chemical Society.

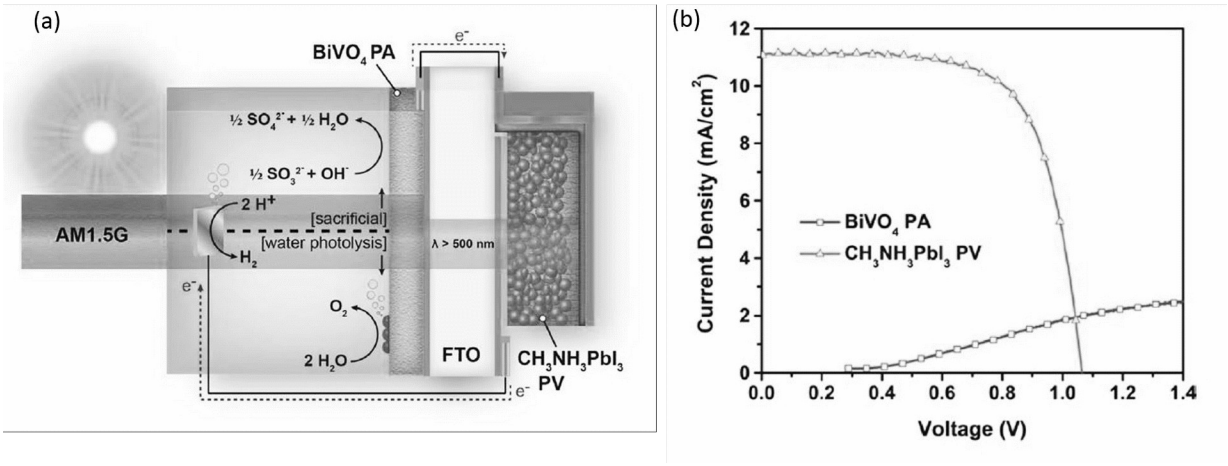

Figure 9. (a) Schematic diagram of the tandem $CoPi/BiVO_4{-}CH_3NH_3PbI_3$ device for solar water splitting, (b) Load curve of the J−V characteristics of CoPi/BiVO4

photoanode and $CH_3NH_3PbI_3$ solar cell in 1 M KPi solution under 1 SUN. Reproduced with permission.[43] Copyright 2015, American Chemical society.

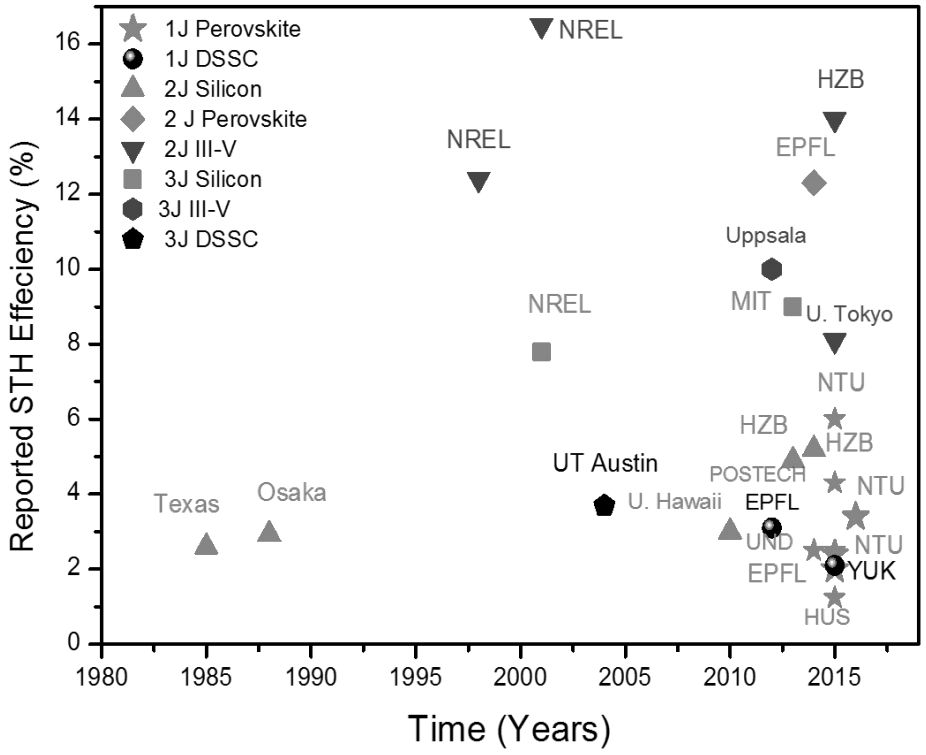

Figure 10. Selected reported solar to hydrogen (STH) conversion efficiencies of PV-PEC configuration under 1 sun illumination conditions. All STH efficiencies are as reported here the original publications.[10, 16, 22, 34, 41, 42, 44-47, 59, 61, 64-67]

2.3. Photovoltaic-Electrocatalyst (PV-EC) Structure

PV-EC is the simplest configuration and has the highest potential for commercialization. In this approach, the water splitting anode and cathode is connected with a multijunction solar cell or a few solar cells in series to split water without any external bias. However, efficient, stable and economical friendly electrode materials need to discover which can split water with minimum overpotential. Early research focused on multi-junctions Si, III-V, and DSSC PV based tandem devices. Those devices are complex in terms of number of solar cell used and poor STH efficiencies. More recently, perovskite PV systems based tandem devices were reported with high STH efficiency. Earlier, Y yamada et al demonstrated a triple junction Si wired with a Co–Mo cathode and FeNiO anode were durable for more than 18 h and achieved STH η of approximately 2.5%.[68] Yamane et al. showed a tandem cell consisted of a multi-junction Si based PV cell and an electrolyzer with RuO_2 anode and Pt cathode, which exhibit STH efficiency of 2.3%.[69] Reece et al. demonstrated slightly higher STH efficiency of 4.7% by using a triple-junction a-Si PV cell and an electrolyzer containing NiMoZn based cathode and cobalt oxide based anode.[66] Cox et al., designed a tandem cell with a triple-junction a -Si PV cell integrated with an NiMoZn cathode and an NiBi anode with a notable STH efficiency of 10%.[65] May et al. demonstrated a III-V based tandem device, in which a GaInP/GaInAs photovoltaics connected in series with Rh and RuO_2 based electrodes with a STH efficiency of 14%.[70] Rau et al. substituted the Rh/RhO_2 electrolyzer with a proton exchange membrane (PEM) electrolyzer, while using GaInP/GaInAs photovoltaics. This configuration exhibit higher STH efficiency of 16.8%.[71] Licht et al reported an extraordinary PV-EC tandem device by combining a III-V PV with an elecctrolyzer containing RuO_2 anode and Pt cathode in 1 M $HClO_4$ electrolyte with a notable STH efficiency of 18.3% under 1 sun illumination.[72] Verlage et al. fabricated a monolithic wireless tandem device consisting of an

NiMo/GaAs/$GaInP_2$/TiO_2/Ni structure for sustained unassisted solar driven overall water splitting with STH efficiency of 8.6%.[67] Lately, a III-V based tandem device shows extra ordinary STH efficiency of 30%. This system contains two polymer electrolyte membrane electrolyzers in tandem with a triple-junction InGaP/GaAs/GaInNAsSb solar cell, which produces more than enough voltage to drive electrolyzer.[73] More recently, perovskite PV cells got more attention for the PV-EC tandem cell because of their high open circuit potential and simple solution processed fabrication technique.

A highly efficient and low-cost water splitting device by using a double-junction perovskite ($CH_3NH_3PbI_3$) PV cell and a bifunctional earth-abundant NiFe layered double hydroxide catalyst was reported by Gratzel's group, as shown in Figure 11. The STH efficiency reached 12.3%.[44]

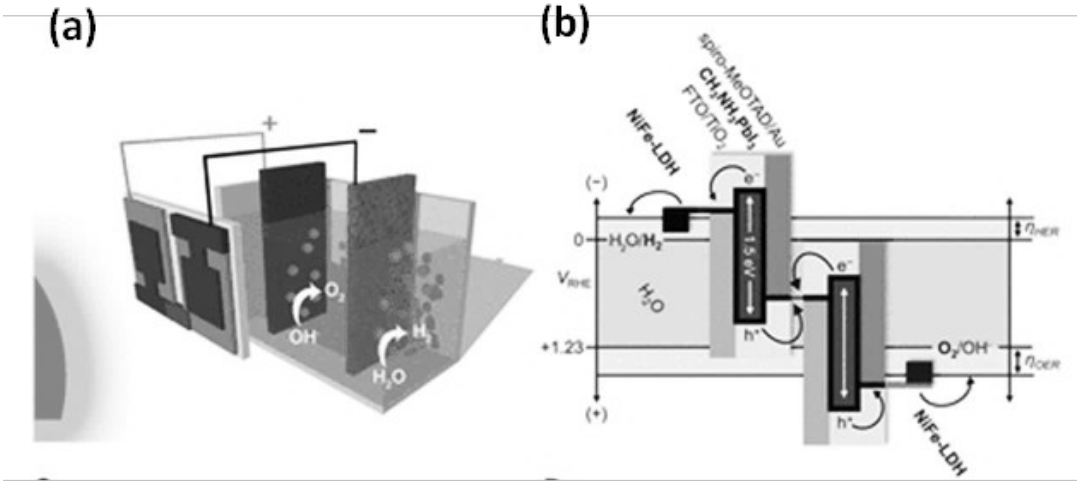

Figure 11. Photovoltaic-electrosynthetic approach of Luo et al. for overall water splitting with an efficiency of 12.3%. Two side-by-side CH3NH3PbI2 cells were used; they were wired to NiFe hydrogen and oxygen evolution catalysts. Reproduced with permission.[44] Copyright 2014, Science.

Halide perovskite got more attention in past few years from research community and achieved an open circuit potential of 1.1 to 1.5 V with a power conversion efficiency of 22.1% reported for $CH_3NH_3PbI_3$.[74] Rashid bin et al, demonstrated a bifunctional metal free nitrogen doped reduced graphene oxide/nitrogen doped carbon nanotube (NrGO/NCNT) hybrid electrocatalyst for hydrogen and oxygen evolution reaction in an alkaline electrolyte (1M KOH) in tandem with perovskite solar cell for the overall water splitting. This system exhibits a solar to hydrogen conversion efficiency of 9.02% (Figure 12).[75] They mentioned the high activity and bifunctional nature of their catalyst is due to the nitrogen doping. They have further improved the power conversion efficiency of their hybrid solar cell by arranging perovskite at the top and polymer electrode as the bottom subcell.

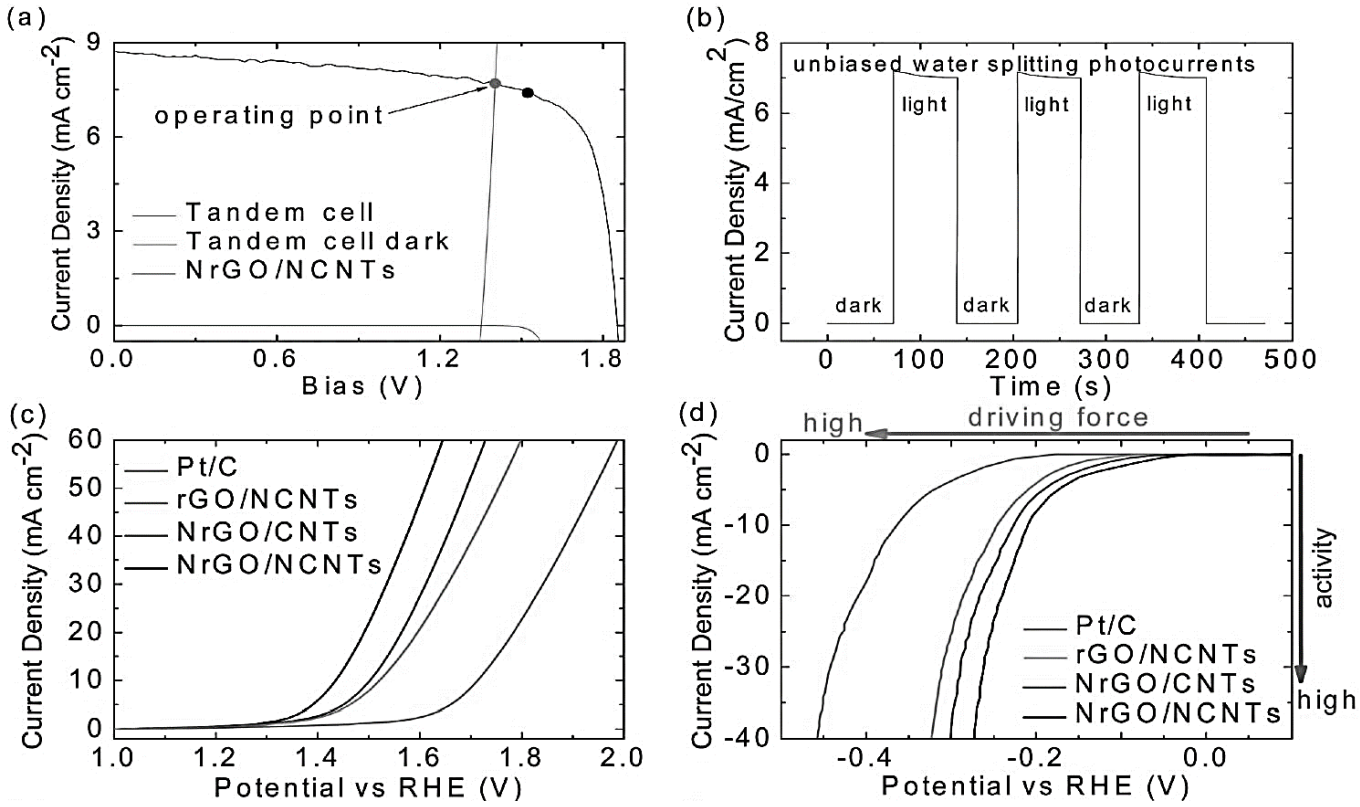

Figure 12. (a) Load curve analysis shows the operating point of a PEC cell as the intersection of the J–V curve of the hybrid tandem perovskite solar cell and the J-V curve of the electrocatalysts. (b) Current density–time curve of the integrated PEC

water splitting without external bias under chopped illumination AM 1.5G 100 $mWcm^{-2}$. (c) OER characteristics of different electrocatalysts in a three-electrode configuration. (d) HER curves comparing their electrocatalytic activity in a three-electrode configuration in a 1M KOH electrolyte. Reprinted with the permission of Royal Society of Chemistry.[75] Copyright @2016.

3. EC/PEC-PV approach for CO_2 reduction

Photo/Electrochemical CO_2 reduction reaction is even more challenging than the water splitting reaction because of multiple electrons requirement to produce hydrocarbons and oxygenates and high overpotential due to kinetic losses. For CO_2 reduction reaction, minimum 3-4 volt is required, which corresponds to the 6-8 silicon solar cells. Perovskite solar cells would help to reduce the complexity and fabrication cost of CO_2 reduction tandem cell due to its high open circuit voltage. Schreier et al. reported CO_2 reduction over a perovskite PV-electrochemical device; the integrated three perovskite solar cells with an electrochemical cell consisting of an IrO_2 anode and an Au cathode, which achieved 7% solar-to-CO conversion efficiency (Figure 13).[76] Arai et al from Toyota center demonstrated a simple CO_2 reduction monolithic device (Figure 14).[77] The device is composed of a porous ruthenium complex polymer (p-RuCP) as a CO_2 reduction catalyst, iridium oxide (IrOx) anode for water oxidation, and a triple-junction of amorphous silicon-germanium. This device exhibits a solar to chemical conversion efficiency of 4.6%, while formate was the only product.

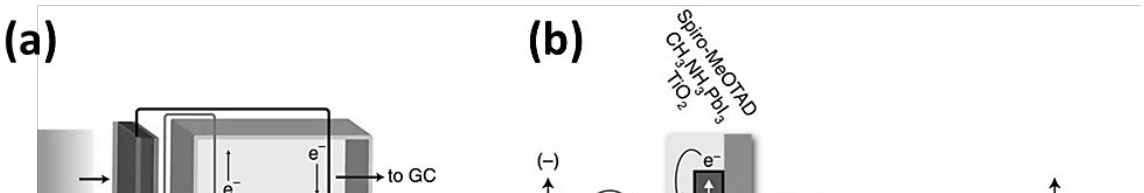

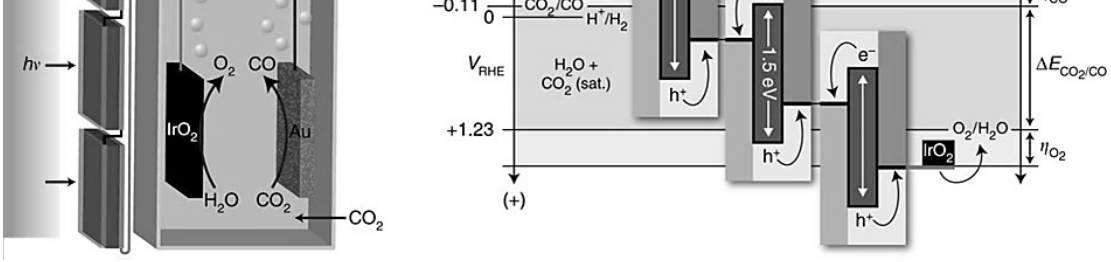

Figure 13. (a) Schematic of a triple junction perovskite solar cell with FeNiOx bifunctioanal layer electrocatalyst for solar assisted overall water splitting, (b) Thin film Photovoltaic-electrosynthetic approach of Scheier et al. 93for solar-driven CO_2 reduction. Three side-by-side $CH_3NH_3PbI_2$ cells were used; they were wired to an Au cathode for reduction of CO_2 to CO and to an IrO_2 anode for water oxidation. Reproduced with permission.[76] Copyright 2015, Nature Publishing Group.

Different type of catalyst materials such as metal electrodes, semiconducting photoelectrodes, metal complexes, molecular catalysts have been discovered to perform the CO_2 reduction reaction. However, the theoretically predicted efficiencies are still far from the achieved efficiencies because of the high overpotential, slow rate of reaction, sluggish kinetics and poor catalyst stability. Nevertheless, there have been a few reports of solar driven CO_2 reduction with solar to fuel efficiencies in the 1-5% range; in all cases, $2e^-$ products like CO or formate were produced.

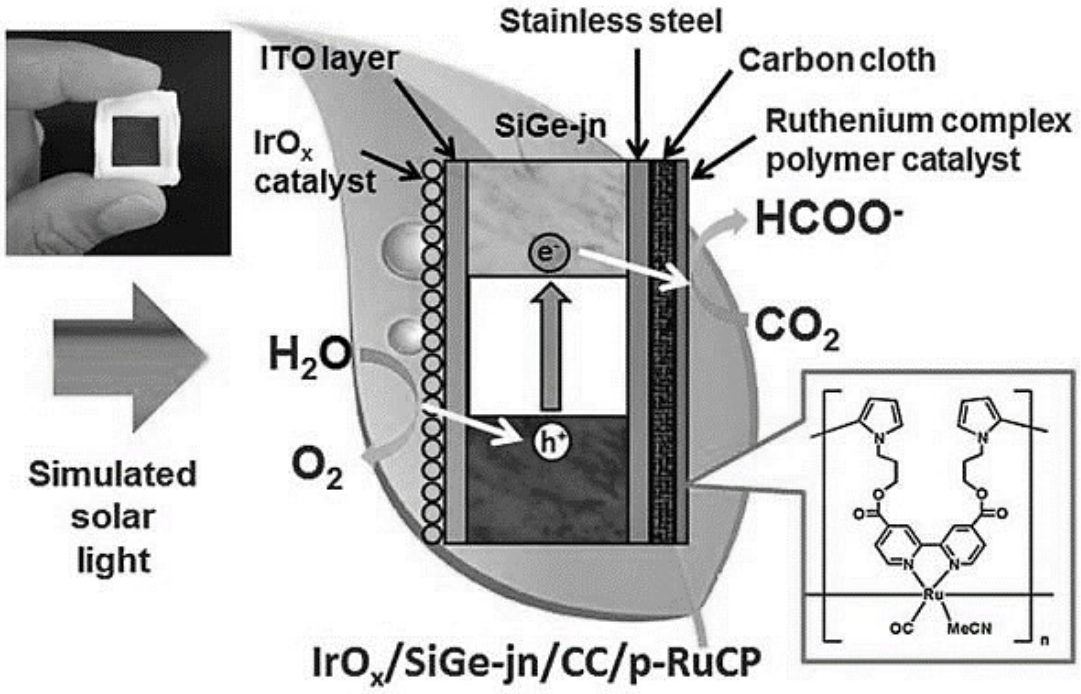

Figure 14. Schematic diagram of the IrOx/SiGe-jn/CC/p-RuCP monolithic device for CO2 photoreduction. Reprinted with permission.[77] Copyright 2015, Royal Society of Chemistry.

Recently, jeong Jang reported an Au/ZnO/ZnTe/CdTe core−shell nanorod array photocathode, cobalt−bicarbonate anode and a $CH_3NH_3PbI_3$ perovskite solar cell in tandem for solar assisted CO_2 reduction.[78] This device harvest light efficiently, as photocathode absorb higher energy photons (>2.14 eV) and perovskite solar cell absorbs lower energy photons (>1.5 eV). Although this device shows only CO with nominal solar to CO conversion efficiency of 0.35% and a solar to fuel conversion efficiency exceeding 0.43% including H_2 (Figure 16). Finally, this device performance was reduced by nearly 30% within 3 hrs.[78]

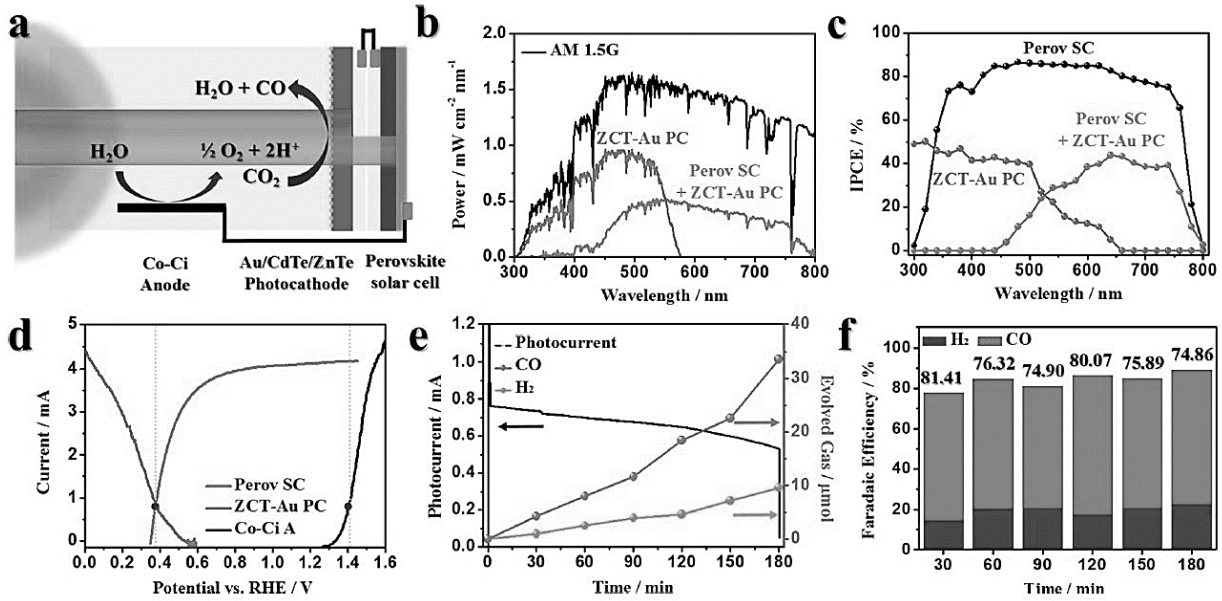

Figure 15. (a) Schematic of a tandem cell comprising of ZnO/ZnTe/CdTe-Au NR photocathode, cobalt bicarbonate (Co-Ci) and perovskite solar cell for photoelectrochemical CO_2 reduction, (b) incident photons of AM 1.5G spectrum by two light absorbers. (c) IPCE responses of photocathode, perovskite solar cell, and the tandem device. The IPCE of photocathode was measured at −0.11 VRHE. (d) J−V curves of ZCT-Au photocathode and Co-Ci anode measured in three-electrode configuration with overlaid response of the solar cell in the stacked tandem device. (e) Chronoamperometry and time-profiled production of CO and H_2 for 3 h in the tandem device. (f) Faradaic efficiencies of CO and H2 during 3 h in the tandem cell with a CO2-saturated KHCO3 electrolyte under simulated 1 sun illumination. Reprinted with permission.[78] Copyright 2016, American Chemical Society.

References

[1] D. J. C. MacKay, Philosophical Transactions of the Royal Society of London A: Mathematical, Physical and Engineering Sciences 2013, 371; I. E. A. (IEA), 2015; B. E. Outlook, BP, 2016; R. E. P. N. F. s. Century, 2015.
[2] S. C. Program, 2015; S. Solomon, G.-K. Plattner, R. Knutti, P. Friedlingstein, Proceedings of the National Academy of Sciences 2009, 106, 1704.
[3] Y. Tachibana, L. Vayssieres, J. R. Durrant, Nature Photonics 2012, 6, 511; M. G. Walter, E. L. Warren, J. R. McKone, S. W. Boettcher, Q. Mi, E. A. Santori, N. S. Lewis, Chemical Reviews 2010, 110, 6446.
[4] J. Keable, B. Holcroft, in *Photoelectrochemical Hydrogen Production*, (Eds: R. van de Krol, M. Grätzel), Springer US, Boston, MA 2012, 277.
[5] J. Barber, Chemical Society Reviews 2009, 38, 185.
[6] A. Listorti, J. Durrant, J. Barber, Nat Mater 2009, 8, 929.
[7] C. Liu, B. C. Colón, M. Ziesack, P. A. Silver, D. G. Nocera, Science 2016, 352, 1210.
[8] T. Bak, J. Nowotny, M. Rekas, C. C. Sorrell, International Journal of Hydrogen Energy 2002, 27, 991.
[9] D. R. Gamelin, Nat Chem 2012, 4, 965; C. R. Cox, J. Z. Lee, D. G. Nocera, T. Buonassisi, Proceedings of the National Academy of Sciences of the United States of America 2014, 111, 14057; H. Doscher, J. F. Geisz, T. G. Deutsch, J. A. Turner, Energy & Environmental Science 2014, 7, 2951.
[10] T. J. Jacobsson, V. Fjallstrom, M. Sahlberg, M. Edoff, T. Edvinsson, Energy & Environmental Science 2013, 6, 3676.
[11] J. Ronge, T. Bosserez, D. Martel, C. Nervi, L. Boarino, F. Taulelle, G. Decher, S. Bordiga, J. A. Martens, Chemical Society Reviews 2014, 43, 7963.
[12] G. W. Crabtree, M. S. Dresselhaus, M. V. Buchanan, Physics Today 2004, 57, 39.
[13] M. Grätzel, Nature 2001, 414, 338.
[14] M. A. Butler, D. S. Ginley, Journal of Materials Science 1980, 15, 1.
[15] J. Brillet, M. Cornuz, F. L. Formal, J.-H. Yum, M. Grätzel, K. Sivula, Journal of Materials Research 2010, 25, 17.
[16] J. H. Kim, Y. Jo, J. H. Kim, J. W. Jang, H. J. Kang, Y. H. Lee, D. S. Kim, Y. Jun, J. S. Lee, ACS Nano 2015.
[17] Z. Chen, T. F. Jaramillo, T. G. Deutsch, A. Kleiman-Shwarsctein, A. J. Forman, N. Gaillard, R. Garland, K. Takanabe, C. Heske, M. Sunkara, E. W. McFarland, K. Domen, E. L. Milled, H. N. Dinh, Journal of Materials Research 2010, 25, 3.
[18] J. W. Ager, M. R. Shaner, K. A. Walczak, I. D. Sharp, S. Ardo, Energy & Environmental Science 2015, 8, 2811.
[19] A. J. Nozik, Applied Physics Letters 1976, 29, 150.
[20] L. M. Peter, Chemical Reviews 1990, 90, 753.
[21] P. S. Bassi, Gurudayal, L. H. Wong, J. Barber, Physical Chemistry Chemical Physics 2014.
[22] O. Khaselev, J. A. Turner, Science 1998, 280, 425.

[23] J. A. Turner, Science 2004, 305, 972; H. Dotan, N. Mathews, T. Hisatomi, M. Grätzel, A. Rothschild, The Journal of Physical Chemistry Letters 2014, 5, 3330.
[24] J. Brillet, J.-H. Yum, M. Cornuz, T. Hisatomi, R. Solarska, J. Augustynski, M. Graetzel, K. Sivula, Nat Photon 2012, 6, 824.
[25] J. R. Bolton, Solar Energy 1996, 57, 37; A. Singh, L. Spiccia, Coordination Chemistry Reviews 2013, 257, 2419.
[26] Y. Lin, G. Yuan, R. Liu, S. Zhou, S. W. Sheehan, D. Wang, Chemical Physics Letters 2011, 507, 209.
[27] B. D. Alexander, P. J. Kulesza, I. Rutkowska, R. Solarska, J. Augustynski, Journal of Materials Chemistry 2008, 18, 2298.
[28] X. Chen, S. Shen, L. Guo, S. S. Mao, Chemical Reviews 2010, 110, 6503.
[29] A. Kudo, Y. Miseki, Chemical Society Reviews 2009, 38, 253.
[30] L. Kavan, M. Grätzel, Electrochimica Acta 1995, 40, 643.
[31] J. H. Park, A. J. Bard, Electrochemical and Solid-State Letters 2005, 8, G371.
[32] K. Shin, J.-B. Yoo, J. H. Park, Journal of Power Sources 2013, 225, 263; N. J. Cherepy, G. P. Smestad, M. Grätzel, J. Z. Zhang, Journal of Physical Chemistry B 1997, 101, 9342; J. E. Kroeze, T. J. Savenije, J. M. Warman, Journal of the American Chemical Society 2004, 126, 7608.
[33] R. H. Gonçalves, L. D. T. Leite, E. R. Leite, ChemSusChem 2012, 5, 2341; Y. Pihosh, I. Turkevych, K. Mawatari, T. Asai, T. Hisatomi, J. Uemura, M. Tosa, K. Shimamura, J. Kubota, K. Domen, T. Kitamori, Small 2014, 10, 3692; M. R. Shaner, K. T. Fountaine, S. Ardo, R. H. Coridan, H. A. Atwater, N. S. Lewis, Energy and Environmental Science 2014, 7, 779; Y. Pihosh, I. Turkevych, K. Mawatari, J. Uemura, Y. Kazoe, S. Kosar, K. Makita, T. Sugaya, T. Matsui, D. Fujita, M. Tosa, M. Kondo, T. Kitamori, Scientific Reports 2015, 5, 11141.
[34] R. H. Coridan, M. Shaner, C. Wiggenhorn, B. S. Brunschwig, N. S. Lewis, Journal of Physical Chemistry C 2013, 117, 6949.
[35] K. Maeda, K. Domen, MRS Bulletin 2011, 36, 25.
[36] J. H. Kennedy, K. W. Frese Jr, Journal of the Electrochemical Society 1978, 125, 709; F. Le Formal, N. Tetreault, M. Cornuz, T. Moehl, M. Gratzel, K. Sivula, Chemical Science 2011, 2, 737; Y. Ling, G. Wang, D. A. Wheeler, J. Z. Zhang, Y. Li, Nano Letters 2011, 11, 2119; P. Zhang, A. Kleiman-Shwarsctein, Y.-S. Hu, J. Lefton, S. Sharma, A. J. Forman, E. McFarland, Energy & Environmental Science 2011, 4, 1020; P. Liao, E. A. Carter, Journal of Applied Physics 2012, 112, 013701; L. M. Peter, K. G. U. Wijayantha, A. A. Tahir, Faraday Discussions 2012, 155, 309; S. C. Warren, K. Voïtchovsky, H. Dotan, C. M. Leroy, M. Cornuz, F. Stellacci, C. Hébert, A. Rothschild, M. Grätzel, Nature Materials 2013, 12, 842.
[37] Gurudayal, P. M. Chee, P. P. Boix, H. Ge, F. Yanan, J. Barber, L. H. Wong, ACS Applied Materials & Interfaces 2015, 7, 6852; Gurudayal, S. Y. Chiam, M. H. Kumar, P. S. Bassi, H. L. Seng, J. Barber, L. H. Wong, ACS Applied Materials & Interfaces 2014, 6, 5852.
[38] A. C. Nielander, M. R. Shaner, K. M. Papadantonakis, S. A. Francis, N. S. Lewis, Energy & Environmental Science 2015, 8, 16.
[39] S. Hu, C. Xiang, S. Haussener, A. D. Berger, N. S. Lewis, Energy and Environmental Science 2013, 6, 2984.
[40] K. Zhang, M. Ma, P. Li, D. H. Wang, J. H. Park, Advanced Energy Materials 2016, 6, n/a.
[41] J. Luo, Z. Li, S. Nishiwaki, M. Schreier, M. T. Mayer, P. Cendula, Y. H. Lee, K. Fu, A. Cao, M. K. Nazeeruddin, Y. E. Romanyuk, S. Buecheler, S. D. Tilley, L. H. Wong, A. N. Tiwari, M. Grätzel, Advanced Energy Materials 2015, n/a.

[42] Gurudayal, D. Sabba, M. H. Kumar, L. H. Wong, J. Barber, M. Grätzel, N. Mathews, Nano Letters 2015, 15, 3833.
[43] Y.-S. Chen, J. S. Manser, P. V. Kamat, Journal of the American Chemical Society 2015, 137, 974.
[44] J. Luo, J.-H. Im, M. T. Mayer, M. Schreier, M. K. Nazeeruddin, N.-G. Park, S. D. Tilley, H. J. Fan, M. Grätzel, Science 2014, 345, 1593.
[45] F. F. Abdi, L. Han, A. H. M. Smets, M. Zeman, B. Dam, R. van de Krol, Nat Commun 2013, 4.
[46] P. Dias, M. Schreier, S. D. Tilley, J. Luo, J. Azevedo, L. Andrade, D. Bi, A. Hagfeldt, A. Mendes, M. Grätzel, M. T. Mayer, Advanced Energy Materials 2015, 5, n/a.
[47] S. Y. Chae, S. J. Park, O.-S. Joo, B. K. Min, Y. J. Hwang, Solar Energy 2016, 135, 821.
[48] H. Wang, J. A. Turner, Journal of The Electrochemical Society 2010, 157, F173.
[49] H. Wang, T. Deutsch, J. A. Turner, Journal of The Electrochemical Society 2008, 155, F91.
[50] G. K. Mor, O. K. Varghese, R. H. T. Wilke, S. Sharma, K. Shankar, T. J. Latempa, K.-S. Choi, C. A. Grimes, Nano Letters 2008, 8, 1906.
[51] Y.-H. Lai, D. W. Palm, E. Reisner, Advanced Energy Materials 2015, 5, n/a.
[52] C. Liu, J. Tang, H. M. Chen, B. Liu, P. Yang, Nano Letters 2013, 13, 2989.
[53] C. Ding, W. Qin, N. Wang, G. Liu, Z. Wang, P. Yan, J. Shi, C. Li, Physical Chemistry Chemical Physics 2014, 16, 15608.
[54] J.-W. Jang, C. Du, Y. Ye, Y. Lin, X. Yao, J. Thorne, E. Liu, G. McMahon, J. Zhu, A. Javey, J. Guo, D. Wang, Nature Communications 2015, 6, 7447.
[55] P. Bornoz, F. F. Abdi, S. D. Tilley, B. Dam, R. van de Krol, M. Graetzel, K. Sivula, The Journal of Physical Chemistry C 2014, 118, 16959.
[56] S. Ida, K. Yamada, T. Matsunaga, H. Hagiwara, Y. Matsumoto, T. Ishihara, Journal of the American Chemical Society 2010, 132, 17343.
[57] J. H. Kim, H. Kaneko, T. Minegishi, J. Kubota, K. Domen, J. S. Lee, ChemSusChem 2016, 9, 61.
[58] J.-W. Jang, C. Du, Y. Ye, Y. Lin, X. Yao, J. Thorne, E. Liu, G. McMahon, J. Zhu, A. Javey, J. Guo, D. Wang, Nat Commun 2015, 6.
[59] J. H. Park, A. J. Bard, Electrochemical and Solid-State Letters 2006, 9, E5.
[60] J. K. Kim, K. Shin, S. M. Cho, T.-W. Lee, J. H. Park, Energy & Environmental Science 2011, 4, 1465.
[61] X. Shi, K. Zhang, K. Shin, M. Ma, J. Kwon, I. T. Choi, J. K. Kim, H. K. Kim, D. H. Wang, J. H. Park, Nano Energy 2015, 13, 182.
[62] L. Han, F. F. Abdi, R. van de Krol, R. Liu, Z. Huang, H.-J. Lewerenz, B. Dam, M. Zeman, A. H. M. Smets, ChemSusChem 2014, 7, 2832.
[63] G. Xing, N. Mathews, S. Sun, S. S. Lim, Y. M. Lam, M. Grätzel, S. Mhaisalkar, T. C. Sum, Science 2013, 342, 344; D. Bi, P. Gao, R. Scopelliti, E. Oveisi, J. Luo, M. Grätzel, A. Hagfeldt, M. K. Nazeeruddin, Advanced Materials 2016, 28, 2910.
[64] X. Zhang, B. Zhang, K. Cao, J. Brillet, J. Chen, M. Wang, Y. Shen, Journal of Materials Chemistry A 2015, 3, 21630.
[65] C. R. Cox, J. Z. Lee, D. G. Nocera, T. Buonassisi, Proceedings of the National Academy of Sciences 2014, 111, 14057.
[66] S. Y. Reece, J. A. Hamel, K. Sung, T. D. Jarvi, A. J. Esswein, J. J. H. Pijpers, D. G. Nocera, Science 2011, 334, 645.
[67] E. Verlage, S. Hu, R. Liu, R. J. R. Jones, K. Sun, C. Xiang, N. S. Lewis, H. A. Atwater, Energy & Environmental Science 2015, 8, 3166.

[68] Y. Yamada, N. Matsuki, T. Ohmori, H. Mametsuka, M. Kondo, A. Matsuda, E. Suzuki, International Journal of Hydrogen Energy 2003, 28, 1167.
[69] S. Yamane, N. Kato, S. Kojima, A. Imanishi, S. Ogawa, N. Yoshida, S. Nonomura, Y. Nakato, The Journal of Physical Chemistry C 2009, 113, 14575.
[70] M. M. May, H.-J. Lewerenz, D. Lackner, F. Dimroth, T. Hannappel, Nature Communications 2015, 6, 8286.
[71] S. Rau, S. Vierrath, J. Ohlmann, A. Fallisch, D. Lackner, F. Dimroth, T. Smolinka, Energy Technology 2014, 2, 43.
[72] S. Licht, B. Wang, S. Mukerji, T. Soga, M. Umeno, H. Tributsch, The Journal of Physical Chemistry B 2000, 104, 8920.
[73] J. Jia, L. C. Seitz, J. D. Benck, Y. Huo, Y. Chen, J. W. D. Ng, T. Bilir, J. S. Harris, T. F. Jaramillo, Nature Communications 2016, 7, 13237.
[74] NREL, Vol. 2017, NREL, 2017.
[75] A. R. Bin, M. Yusoff, J. Jang, Chemical Communications 2016, 52, 5824.
[76] M. Schreier, L. Curvat, F. Giordano, L. Steier, A. Abate, S. M. Zakeeruddin, J. Luo, M. T. Mayer, M. Grätzel, Nature Communications 2015, 6, 7326.
[77] T. Arai, S. Sato, T. Morikawa, Energy & Environmental Science 2015, 8, 1998.
[78] Y. J. Jang, I. Jeong, J. Lee, J. Lee, M. J. Ko, J. S. Lee, ACS Nano 2016, 10, 6980.